HHS Public Access

Author manuscript

Immunity. Author manuscript; available in PMC 2016 March 15.

Published in final edited form as:

Immunity. 2014 February 20; 40(2): 235–247. doi:10.1016/j.immuni.2013.11.017.

Tuning of Antigen Sensitivity by TCRT Cell Receptor-Dependent Negative Feedback Controls T Cell Effector Function in Inflamed Tissues

Tetsuya Honda[#1], **Jackson G. Egen**[#1,2], **Tim Lämmermann**[1], **Wolfgang Kastenmüller**[1], **Parizad Torabi-Parizi**[1,3], and **Ronald N. Germain**[1,*]

[1]Lymphocyte Biology Section, Laboratory of Systems Biology, National Institute of Allergy and Infectious Diseases, National Institutes of Health, Bethesda, MD 20892, USA

[3]Critical Care Medicine Department, Clinical Center, National Institutes of Health, Bethesda, MD 20892, USA

[#] These authors contributed equally to this work.

Abstract

Activated T cells must mediate effector responses sufficient to clear pathogens while avoiding excessive tissue damage. Here we have combined dynamic intravital microscopy with *ex vivo* assessments of T cell cytokine responses to generate a detailed spatiotemporal picture of $CD4^+$ T cell effector regulation in the skin. In response to antigen, effector T cells arrested transiently on antigen presenting cells, briefly producing cytokine and then resuming migration. Antigen recognition led to PD-1 upregulation of the programmed death-1 (PD-1) glycoprotein by T cells and blocking its canonical ligand, programmed death-ligand 1 (PD-L1), lengthened the duration of migration arrest and cytokine production, showing that PD-1 interaction with PD-L1 is a major negative feedback regulator of antigen responsiveness. We speculate that the immune system employs a mechanism involving T cell recruitment, transient activation, and rapid desensitization, allowing the T cell response to rapidly adjust to changes in antigen presentation and minimize collateral injury to the host.

Keywords

PD-1; effector T cells; intravital imaging; cytokine production; immune regulation

Introduction

Effector T cells develop from naïve T cell precursors in secondary lymphoid organs upon encountering processed antigen (pMHC ligands) on antigen-presenting cells (APCs). Following activation, clonal expansion, and differentiation, the T cells acquire the capacity to produce distinct sets of effector cytokines and through the expression of specific tissue homing receptors, to access sites of infection or cellular damage via locally inflamed

[*]Correspondence: Ronald N. Germain (rgermain@nih.gov).
[2]Present address: Genentech, 1 DNA Way, MS34, South San Francisco, CA 94080, USA

endothelium (Campbell and Butcher, 2002; Mora et al., 2003) where they play a crucial role in control of microbial infections and tumors and are major contributors to tissue-specific autoimmunity (Swain et al., 2012; Zhu et al., 2010).

Once effector T cells enter into inflamed tissue and recognize their specific antigen on tissue resident APCs, they undergo reactivation, producing effector cytokines that can contribute to host defense by enhancing anti-microbial responses. Local chemokine production by these activated T cells or evoked from neighboring cells can promote further recruitment of immune effectors (Islam and Luster, 2012; Sadik and Luster, 2012). Although these various cells and mediators are crucial to host defense, many of the molecules involved can cause substantial damage to host tissue. Thus, the quality, magnitude, and duration of effector T cell activity in a tissue site must be carefully regulated to provide a useful balance between adequate host protection and acceptable collateral organ damage (Germain et al., 2012; Sancho et al., 2002; Segel and Bar-Or, 1999).

Until recently, analysis of T cell effector activity, especially in peripheral tissues, was mainly indirect. Studies of gene-targeted animals have helped identify specific cytokines involved in protection against certain pathogens and flow cytometry and ELISA-based methods have revealed the relationship between cell phenotype and the capacity to produce these effector molecules, most often after *ex vivo* restimulation (Hafalla et al., 2012; Wilson et al., 2009). A more limited number of studies have examined cytokine production by T cells without such restimulation (Reinhardt et al., 2003). Static *in vivo* imaging with staining for both cell phenotypic markers and cytokines has also contributed to our understanding of the location and magnitude of effector T cell activity in tissues (Egen et al., 2011).

While this prior work has provided important insights about effector T cells and their behavior in antigen-rich settings, it lacks an understanding of the spatiotemporal dynamics of this limb of the immune system, in particular, the time evolution of the relationships among antigen recognition, cytokine production, and cell movement. The application of 2-photon (2P) microscopy to intravital imaging of immune cells has provided a key tool for such analysis. Initially applied to the behavior of naïve T cells in secondary lymphoid tissues (Bousso and Robey, 2003; Mempel et al., 2004; Miller et al., 2002; Stoll et al., 2002), this method has more recently been used to analyze effector T cells in various peripheral sites (Bartholomaus et al., 2009; Beattie et al., 2010; Egen et al., 2011; Egen et al., 2008; Fife et al., 2009; Filipe-Santos et al., 2009; Kawakami et al., 2005; Kim et al., 2009; Matheu et al., 2008; Schaeffer et al., 2009; Wilson et al., 2009). A common observation is the rapid movement of activated T cells within dense tissue and their migration arrest when contacting cells presenting antigen of suitable quality and quantity. In our studies involving a BCG-induced liver granuloma model (Egen et al., 2011; Egen et al., 2008), we reported the close relationship between motility state and effector function, with the fraction of antigen-specific cells showing antigen-induced arrest of migration correlating with the fraction producing interferon-gamma (IFN-γ). However, these and other investigations have not adequately explored the evolution of the effector response over longer time intervals for two major reasons; first, the lack of a method for narrowly defining the moment of initial antigen contact in the tissue so that the kinetics of the cytokine response can be linked to the onset of antigen-induced signaling, and second, the inability to image long enough to observe the

temporal arc of the functional response induced by such antigen stimulation. Without this information, critical questions about effector cell behavior such as what fraction of antigen-specific cells participate in a response, whether actively migrating cells are high-rate cytokine producers, and the mechanisms controlling eventual T cell disengagement from antigen-specific contacts with APCs all remain unanswered.

To address these issues, we have combined 2P intravital microscopy with more traditional cellular analytical methods to examine the spatiotemporal behavior of $CD4^+$ effector T cells in a skin delayed-type hypersensitivity (DTH) model. Two key elements of the study were the use of a method that synchronizes the onset of antigen presentation to T cells within an inflamed tissue site and the extension of the imaging analysis to a period of up to 10 hrs. Using these methods, we found that effector T cells exhibited reduced velocity and high IFN-γ production immediately after TCR engagement but gradually recovered motility and ceased effector activity over several hours through a process that was independent of marked decline in antigen presentation at the inflamed site. During this period, programmed death-1 (PD-1) expression on effector T cells increased and blockade of PD-1 activity using an anti-programmed death-ligand 1 (PD-L1) antibody delayed the recovery of motility and prolonged the duration of cytokine secretion. These results indicate that effector T cells undergo rapid tuning of their sensitivity to antigenic stimulation, in part through T cell receptor (TCR)-dependent negative feedback control afforded by increased PD-1 expression on T cells. We propose that this mechanism constrains tissue damage by adapting the magnitude of the effector response to the ambient amounts of antigen present within the inflamed site. These findings suggest a critical role for central memory cells in generating a continuous source of new ‘virgin’ effectors, which, upon sequential immigration into the inflamed site, can sense dynamic fluctuations in antigen display and generate a proportional effector response.

Results

Both antigen-induced signaling and tissue anatomy regulate motility of effector T cells in skin

To explore the dynamic behavior and functionality of effector T cells in a peripheral inflamed tissue in which we could control the display of cognate antigen and conduct long-term dynamic *in situ* imaging, we developed a DTH model in which an adoptively transferred antigen-specific population of $CD4^+$ T cells could be observed in the skin (Fig. 1A) (Kearney et al., 1994). Naïve TCR transgenic OT-II-Rag-eGFP T cells (OT-II T cells) were transferred into syngeneic, albino recipient mice, to avoid tissue damage due to absorption of laser excitation by melanin granules (Masters et al., 2004). These animals were then immunized with complete Freund’s adjuvant (CFA) containing keyhole limpet hemocyanin (KLH) and the OT-II TCR-specific peptide ovalbumin 323-329 (OVA323). Seven days later, the ear skin was challenged with an intradermal injection of either KLH or KLH plus ovalbumin protein (OVA). Immunization and challenge with KLH evoked a DTH response that led to robust ear swelling 24-48 hrs later. Mice with primed OT-II T cells that were re-challenged with KLH+OVA developed only a marginally increased ear swelling response as compared to those re-challenged with KLH alone, suggesting that the majority

of inflammation is driven by the response to KLH (Figure. S1). The number of effector OT-II T cells recruited into the inflamed ear at 12 and 60 hrs after the challenge was not substantially influenced by presence of specific antigen at these assay times (Fig. 1B,C), revealing that activated effector T cells were recruited to and retained in inflammatory skin lesions with limited dependence on their antigen specificity, consistent with our previous report (Egen et al., 2011). This homing characteristic allowed us to compare the behavior of effector OT-II T cells in KLH-challenged skin vs. KLH+OVA-challenged skin in the same animal and state of immune response, with the only major variable being the local presence or absence of specific antigen.

Using this system, we first characterized the localization and migration of OT-II T cells in inflamed skin in the absence of cognate antigen. Immunofluorescence analysis of skin sections showed a large number of recruited OT-II T cells in the dermis surrounded by a rich network of major histocompatibility complex (MHC) class II^+ cells, representing potential APCs (Fig. 1D). In these fixed tissue sections we also observed smaller numbers of OT-II T cells in an epidermal compartment. We utilized intravital imaging to investigate the dynamic behavior of the dermal and epidermal OT-II T cell populations, performing the study in recipient mice that constitutively express dsRed in all cell types (Ubi-dsRed) so as to visualize the surrounding cellular environment. These studies revealed that the effector T cells were relatively free to move throughout the inflamed dermal environment with its looser mass of connective tissue and cells, whereas epidermal T cells appeared highly constrained by their surroundings, showing substantial shape changes as they squeezed through small openings between tightly adherent keratinocytes (Fig. 1E and Movie S1,S2). As a consequence, the mean velocity of T cells in the epidermis was substantially reduced compared to T cells migrating in the dermis (Fig. 1F), consistent with previously reports (Ariotti et al., 2012; Chodaczek et al., 2012; Gebhardt et al., 2011). These findings emphasize the critical importance of imaging tissue structure along with immune cells of interest in interpreting data on migration dynamics control, and provide insight relevant to effector cell clearance of epidermal infections. Given the limited motility of OT-II T cells in the epidermis and our interest in relating migratory dynamics to effector function, we focused on examination of dermal T cell populations for the remainder of our study.

We next investigated the effect of specific antigen on OT-II T cell migration in the inflamed dermis. Previous studies have demonstrated that effector T cells arrest migration when they contact a high potency antigen available at adequate density on tissue APC (Bartholomaus et al., 2009; Beattie et al., 2010; Egen et al., 2011; Fife et al., 2009; Filipe-Santos et al., 2009; Kawakami et al., 2005; Kim et al., 2009; Matheu et al., 2008; Schaeffer et al., 2009; Wilson et al., 2009). In agreement with these previous results and the abundance of potential APC in the dermis, at 12 hrs and 24 hrs after challenge with KLH+OVA, OT-II T cells in the dermis had a substantially lower mean velocity than OT-II T cells in the ear given only KLH (Fig. 1G and Movie S3). In the absence of cognate antigen recognition (KLH challenge only), we observed a change in OT-II cell velocity as the DTH response progressed. Cell velocity increased slightly from 12 to 24 hours after KLH challenge but then decreased at later time points, presumably due to the changing inflammatory environment. By 48 hrs after the challenge, OT-II T cells in KLH+OVA challenged ears had regained motility close to that of OT-II T cells in the KLH challenged ear.

Temporal synchronization of antigen presentation reveals that effector T cell motility and cytokine production are anti-correlated

Our observations demonstrating that at an inflamed site in the presence of antigen, effector OT-II T cell arrest their migration early in the response but then display heterogeneity in their motility as the response ensues, led us to investigate the process by which T cells engage with APCs, generate effector responses, and then disengage from APC contact, resuming migration. To generate a synchronized population of effector T cells in which the moment of antigen recognition is known within a narrow window, co-ordinate throughout the population, and observable during the imaging session, we developed a modified DTH system (Fig. 2A). Mice were immunized with KLH+OVA323 in CFA after transfer of naïve OT-II T cells and then challenged in the ear with KLH alone 7 days later to recruit OT-II effector T cells in the absence of cognate antigen. To synchronously induce and monitor activation of these T cells, OVA323 peptide was injected i,v, and OT-II T cell motility changes observed by intravital microscopy (Egen et al., 2011; Waite et al., 2011). Before antigen injection or following injection of an irrelevant peptide antigen, OT-II T cells moved rapidly with a mean velocity of ~5μm/min (Fig. 2B). Within 1 minute of OVA323 injection, antigen-specific T cells showed migration arrest, with higher doses of injected peptide leading to greater declines in the mean velocity (Fig. 2B and Movie S4), due primarily to more T cells arresting completely as the antigen dose increased (Figure. S2). To determine how these motility changes correlated with T cell effector activity, we examined the appearance of intracellular cytokine (IFN-γ) beginning at 2 hrs after peptide administration, using a previously described system in which T cells are analyzed directly *ex vivo*, in the absence of re-stimulation (Egen et al., 2011). The fraction of OT-II T cells producing IFN-γ increased in parallel with the change in the fraction of arrested cells (Fig. 2C, D), in accord with our previous findings (Egen et al., 2011).

Over the course of these acute peptide administration studies we found that the antigen-arrested T cells began to regain motility several hours later (Fig. 2B). To extend these findings, we studied effector OT-II T cell dynamics in the skin of animals given 100μg of OVA323 peptide and subjected to 10 hrs of continuous imaging. These analyses confirmed that antigen-induced migration arrest was transient, with cells beginning to regain motility 1-2 hrs after peptide injection and nearing their original speeds by 6-8 hrs (Fig. 2E and Movie S4). We also examined the migration of individual T cells (Figure. S3). Individual T cells rapidly arrested following peptide administration, but the subsequent recovery period was heterogeneous, with some cells regaining motility within 30 minutes and others remaining arrested for several hours. A rare population of T cells never regained motility during the imaging period. Following an extended arrest period induced by peptide injection, most T cells showed a prolonged recovery, oscillating between periods of brief arrest and motility, suggestive of additional TCR stimulation, before regaining a migration pattern similar to what was observed in the absence of antigen.

Ex vivo analysis of IFN-γ production without re-stimulation under the same experimental conditions showed an inverse relationship between migration and effector activity; T cells reached a peak of IFN-γ production by 2 hrs after initial antigen contact during which time they showed migration arrest; they then ceased making cytokine as they regained motility

over the next several hours (Fig. 2E). Given that the velocity change largely reflected individual cells transiting between the arrested and motile states (Figure. S3), these data are consistent with T cells making cytokine during prolonged contacts with APC and ending cytokine production as they transition back to the migratory state.

Intact antigen presentation after the regain of T cell motility

This 'single cycle' response of effector T cells in an inflamed tissue was unexpected and led us to investigate the molecular mechanisms underlying this behavior. Two major possibilities were considered; first, the loss of displayed pMHC ligands and the associated TCR 'stop signal' (Dustin, 2004) and second, a change in the response of the T cells to continued antigen display. We examined the first possibility by using a new cohort of adoptively transferred OT-II effector cells as a sensitive indicator of residual dermal antigen display when the *in situ* cohort of OT-II cells had regained motility several hours after antigenic stimulation. If we observed migration arrest of this new OT-II cohort but not of control effector T cells of a different specificity, this would exclude loss of antigenic signal as the basis of the termination of cytokine production and regain of migratory behavior. A DTH response to KLH was induced as before and the mice injected with OVA323 peptide to induce synchronized TCR activation. Nine hours after peptide injection, when the initial cohort of endogenously primed OT-II cells had regained motility, *in vitro* generated OT-II effector T cells and control p25 effector T cells recognizing the mycobacterial antigen, antigen-85b (Ag85b), were labeled with different dyes and adoptively transferred into the OVA323-challenged or saline-treated animals (Fig. 3A). In the OVA peptide-injected recipients, the *in situ* primed OT-II effector T cells had almost fully regained motility and moved at nearly the same velocity as the control transferred p25 T cells (Fig. 3B,C). In clear contrast, a large fraction of the newly transferred OT-II effector T cells showed markedly reduced velocity as compared to activated OT-II and p25 cells transferred into animals without OVA323 peptide injection, the migration-inhibited OT-II T cells that had recovered motility at this time point in peptide–treated animals, or p25 control cells in the same tissue (Fig. 3B-D, and Movie S5). These results indicated that dermal APCs still presented enough antigen to mediate specific migration arrest even 12 hrs after peptide administration, raising the possibility that dissociation of previously activated effector T cells from APCs and cessation of cytokine production beginning a few hours after initiation of peptide-dependent antigen presentation was linked to changes in the T cell response to an otherwise activating level of presented antigen.

PD-1 expression on T cells is increased after antigen-induced arrest

Multiple T cell-intrinsic processes could regulate the termination of TCR signaling and subsequent disengagement from APCs. The most direct mechanisms would involve antigen-induced down-modulation of the TCR (Utzny et al., 2006; Valitutti et al., 2010), the CD4 co-receptor (Schreiber et al., 2010) or other receptors mediating cell adhesion or regulating chemokine sensitivity. Alternatively, several T cell surface molecules have been proposed to actively inhibit antigen-induced stopping and promote T cell motility, including CTLA4 (Downey et al., 2008; Schneider et al., 2006; Schneider et al., 2008), and PD-1 (Fife et al., 2009; Schreiber et al., 2010). The surface expression of both CTLA4 and PD-1 is increased upon TCR signaling, so both were candidates for molecules that might contribute to time-

dependent desensitization and loss of TCR-induced migration arrest and cytokine production. We therefore looked for changes in expression of various surface molecules on OT-II T cells after antigen-induced arrest (Fig. 4A). PD-1 but not CTLA4, Lag3 (another putative negative regulatory molecule), TCR, CD28, the integrins LFA-1,and ICAM, or various chemokine receptors showed substantial expression change within 3 hrs after antigen-induced arrest. For PD-1, there was a significant membrane increase in close kinetic correlation with the loss of migration arrest and effector activity (Fig. 4B). Given that the PD-1 ligands PD-L1 and PD-L2 are well expressed on skin $CD11c^{+}$ $MHCII^{+}$ cells (Figure. S4) and that these cells can serve as APCs for effector T cells during DTH responses (Movie S6), these results suggested the possibility that engagement of an increasing pool of surface PD-1 might play a role in the disengagement of T cells from APC and the regain of motility that begins a few hours after antigen activation in the skin.

Blockade of PD-L1 slows T cells motility recovery and prolongs cytokine production after antigen-induced arrest

To examine whether PD-1 played a role in regulation of T cell effector behavior after acute antigen activation, we inhibited its interaction with its ligands PD-L1 or PD-L2. Data were recorded in each experimental animal from a single imaging field before and then every hour after acute challenge with OVA323 for up to 8 hrs, allowing examination of the effects of antibody blockade on motility while taking into account animal to animal variability and effects of local differences in tissue structure and phase of the DTH response. In control mice given isotype-matched antibody, the average velocity of the OT-II T cells had recovered to the basal state by 6 hrs after antigen-induced arrest (Fig. 5A). In contrast, anti-PD-L1 antibody treatment prolonged the duration of antigen-induced T cell arrest, with the average mean velocity remaining below baseline for the 6 hrs duration of the imaging session (Fig. 5B). There was no effect of anti-PD-L1 antibody on the velocity of effector T cells in the absence of antigen-specific engagement (data not shown). Administration of anti-PD-L2 antibody (Fig. 5C) or anti-CTLA4 antibody (Fig. 5D) did not result in the same change in motility re-acquisition by the T cells (summarized in Fig. 5E). While a trend towards slower recovery of motility was observed with anti-CTLA4 treatment, careful analysis of the area under the curve for the results shown in Fig. 5E revealed that only anti-PD-L1 treatment had a significant effect on changes in motility following antigen-induced arrest (Fig. 5F). To control for T cell extrinsic effects of anti-PD-L1 treatment, we performed additional experiments using control effector p25 T cells. Mice were transferred with both OT-II-CFP T cells and p25-eGFP T cells, and then immunized with CFA containing OVA323 and Ag85b peptides to generate both types of effector T cells *in situ*. After KLH challenge, both effector populations were observed in the dermis and could be discriminated based on their unique fluorescent protein expression. Mice were treated with either anti-PD-L1 antibody or control isotype antibody, and then injected with OVA323. Antibody treatment did not affect initial antigen-induced arrest (Figure S5). At 8 hrs after OVA323 injection in animals given control antibody, the average velocity of OT-II-CFP T cells was the same as p25-eGFP-T cells, while in mice treated with anti-PD-L1 antibody, the average velocity of OT-II-CFP T cells was significantly lower than that of the p25-eGFP T cells (Fig. 5G,H and Movies S6), confirming that blockade of PD-L1 signaling caused a delay of T cell motility recovery in antigen-responding T cell populations, without affecting

the velocity of bystander populations of effector T cells that were not engaged with APCs. We also examined the effect of anti-PD-L1 treatment on T cell dynamics at 48 hours post-rechallenge with OVA protein. Consistent with our findings using systemic peptide injection, we observed decreased T cell motility and displacement following PD-L1 blockade (Figure S6).

Together, these data suggest that PD-L1 signaling through PD-1 on T cells can actively suppress antigen-driven T cell arrest. Given our previous observations on the anti-correlation of effector T cell motility and cytokine production, we hypothesized that PD-1 engagement with PD-L1 would also affect the temporal pattern of T cell effector function elicited by antigen stimulation. IFN-γ production from OT-II T cells after activation by OVA323 peptide injection was examined with or without anti-PD-L1 antibody administration. At 3 hrs after OVA323 injection, close to the normal peak of the cytokine response, there was no significant difference in the percentage of IFN-γ-producing OT-II T cells between isotype control treated mice and anti-PD-L1 antibody treated mice (Fig. 6B). However, 8 hrs after OVA323 injection when the cells had usually regained full motility and largely ceased induced cytokine production, the percentage of IFN-γ-producing cells was significantly higher in anti-PD-L1 antibody treated mice than in control mice (Fig. 6A,C), in accord with the accompanying delay in return to the motile state (Fig. 5B). Thus, PD-1 ligation plays an important role in regulating the temporal evolution of both post-activation T cell migration dynamics and effector activity.

Discussion

Useful adaptive immune T cell responses in tissues involve the emigration of activated lymphocytes from the vasculature across inflamed endothelium into the tissue space. There these effector T cells migrate in search of cells displaying processed antigen in the context of MHCI or MHCII molecules which, when found, allow T cells to engage in host defense through activation of specific effector programs. The ensuing response must be robust enough to clear an invading pathogen but sufficiently restrained so as to prevent excessive tissue damage. To explore how effector T cell activity is controlled dynamically at sites of inflammation, we established a DTH model in which very tight temporal control of initial antigen recognition can be used to investigate the temporal connections between T cell migration, interaction with APC, and effector activity.

Consistent with our prior observations (Egen et al., 2011), we found that T cells rapidly arrest migration in response to antigen challenge, an event tightly linked to effector cytokine production. However, by 2-3 hrs after initiation of TCR signaling, effector cells exited their arrested state and began to migrate in the tissue while ceasing cytokine production. This ‘single cycle’ response behavior occurred even though pMHC ligand density in the tissue was sufficient to cause antigen-specific T cell stopping. Analysis of negative regulatory pathways linked to TCR signaling revealed a major, though not exclusive role, for PD-1 interaction with APC-expressed PD-L1 in actively terminating antigen-induced T cell arrest on APC and limiting the duration of cytokine production.

The effect of antigen recognition on T cell motility has been previously examined *in vitro* and *in vivo* using various imaging modalities. *In vitro*, TCR engagement by strong agonist pMHC ligands at high densities induces a stop signal, with the T cell in tight synaptic connection with the APC membrane (Dustin, 2004; Negulescu et al., 1996). Intravital dynamic imaging first done in a rat experimental allergic encephalomyelitis model has shown that 40 % of transferred myelin basic protein -specific effector T cells become immobile within the central nervous system where their specific antigen exists, whereas almost all cells with an irrelevant TCR migrated vigorously unless their antigen was administered systemically (Kawakami et al., 2005). In several other models, the majority of specific but not unspecific $CD4^+$ or $CD8^+$ effector T cells in tissues or secondary lymphoid organs also stopped migrating in the presence of high amounts of cognate antigen (Azar et al., 2010; Filipe-Santos et al., 2009; Waite et al., 2011), and a similar pattern of TCR-induced migration arrest on strong ligands is seen among thymocytes (Bhakta et al., 2005). In a more limited number of imaging studies, the presence of cognate antigen does not result in a statistically significant change in mean velocity of the antigen-specific population (Filipe-Santos et al., 2009; Kim et al., 2009; Schaeffer et al., 2009), although biological responses of these cells could be measured. This led to the interpretation that transient contact between the T cell and APC is adequate to drive full activation. However, our study in a BCG liver granuloma model has shown clearly that there is a close match in frequency between fully arrested T cells and cytokine-producing T cell in the lesion and that such cells represent only 5-10% of the population (Egen et al., 2011). Linkage of migration arrest and function could be missed in analyses reporting ‘multi-hit’ activation of continuously migrating T cells when looking only at mean velocity metrics under conditions in which only a small fraction of effectors at any moment were engaged in stopping behavior and response.

This issue of whether T cells respond only when arrested on APC or while still migrating is of critical importance in developing an understanding of the range over which cytokines might mediate their effects *in vivo*. Although diffusion or bulk flow in tissue fluid can in principle spread the signal from a cytokine secreted by an activated, arrested effector cell (Muller et al., 2012), migrating cells would clearly have an advantage in distributing such mediators widely in the tissue. This could either be of benefit in limiting infectious spread or detrimental by producing tissue damage at sites distant from foci of infection that require control. The data in the present report are consistent with our findings in the granuloma model (Egen et al., 2011), indicating that effector cells interacting with strong foreign antigens undergo activation while tightly associated with APC and rapidly cease cytokine production and secretion once TCR signaling wanes and contact is lost as migration resumes. Such findings point to a model of host defense in which locally secreted rather than widely distributed cytokines play a predominant role. This does not mean that the effect of a secreted cytokine is limited to just the APC conjugated with the arrested and activated T cells. IFN-γ effects can be measured 80-100 μm from an arrested and activated effector T cell (Muller et al., 2012). This makes biological sense, as the cells in the immediate vicinity of the APC are the most likely to become infected if microbe control is incomplete and hence, raising their resistance to productive infection is a useful host defense strategy.

The upregulation of negative feedback regulators of TCR signaling, especially PD-1, appeared to play the major role in causing strongly arrested and activated T cells to regain motility and cease cytokine production within a few hours of initial antigen contact. Our findings are consistent with previous imaging studies showing that PD-1 interaction with its ligands on APC can limit the capacity of antigen to induce T cell migration arrest and response (Fife et al., 2009) and are further supported by the recent demonstration that PD-1 interactions can inhibit proximal TCR signaling and thus limit the TCR-induced stop signal (Yokosuka et al., 2012). These data stand in contrast to a recent report that PD-1 promotes migration arrest and effector function of splenic $CD8^+$ T cells in a viral infection model (Zinselmeyer et al., 2013); the basis for this difference in findings remains to be determined. We also observed a trend towards a modest decrease in the rate at which T cells regain motility following antigen engagement after blockade of CTLA-4, although these findings were not statistically significant. Nevertheless, a role for CTLA4 in reversing antigen-induced migration arrest of T cells has been described in other circumstances (Downey et al., 2008; Schneider et al., 2006; Schneider et al., 2008) and given its endosomal localization and TCR signaling-induced stabilization on the cell surface (Egen and Allison, 2002; Linsley et al., 1996), it is tempting to speculate that CTLA-4 may also function to sense the extent of antigen engagement and modulate the duration of T cell contacts with APCs.

At first glance, it seems counter-intuitive that activated effector T cells would cut short their response to antigen while the latter persists in amounts adequate for effective stimulation of newly arriving T cells of the same specificity. However, there are several reasons why adaptively decreasing T cell antigen sensitivity could be beneficial to immune responses. Regulatory programs that actively promote disengagement of T cells from APCs may prevent T cells from being trapped around inflamed venules on the first antigen-bearing APC they encounter and thereby promote both the migration of T cells deeper into inflamed tissue. In addition, general considerations of homeostasis as well as explicit modeling have both suggested that the immune system must find a careful balance between effective host defense and the disruption of tissue integrity due to the toxic effects of mediators such as cytokines, enzymes, and reactive oxygen species (Grossman and Paul, 1992; Segel and Bar-Or, 1999). Regulatory mechanisms that rapidly tune down T cell antigen sensitivity to a point that precludes prolonged responses to the antigen density that first evoked the response may provide one solution to this problem. Of course, local desensitization of T cell activation thresholds could also give pathogens a respite from attack if mechanisms do not exist to maintain the T response in the face of continuing infection. We propose that rapid antigen-driven desensitization of T cells at the site of infection combined with a continuous influx of newly generated effector T cells capable of delivering a transient burst of activity, allows for rapidly tuning the potency of T cell responses in co-ordination with fluctuations in antigen display. If antigen presentation is increasing, T cells at the site of infection will be able to respond even with the sensitivity loss that has occurred. If the antigen amount is stable or falling, however, T cells already at the site of infection will cease to participate in the response and continued effector activity will be dependent on newly arriving effector T cells coming from stem cell-like central memory cells (Gattinoni et al., 2011) and capable of being activated by this lower amount of antigen. These cells, produced within draining lymphoid organs, will only be activated upon arrival in the infected tissue to the extent they

are required to drive down pathogen load and no more due to the same desensitization mechanism, thus maximizing tissue viability while effectively defending the host. Seen in this framework, the feedback-controlled, time-limited activity of effector T cells we document here provides insights into how the immune system balances the competing requirements of host defense and tissue homeostasis.

Methods

Mice

C57BL/6 OT-II TCR transgenic RAG1-deficient mice (Barnden et al., 1998) and CD11c-YFP (Lindquist et al., 2004) mice were from Taconic Laboratories. C57BL/6 p25 TCR transgenic RAG1-deficient animals were kindly provided by J. Ernst (New York University School of Medicine, New York) (Wolf et al., 2008). Albino C57BL/6-Tyr$^{c\text{-}2J/c\text{-}2J}$ mice, C57BL/6 ubiquitously expressing eGFP or dsRed (Schaefer et al., 2001; Vintersten et al., 2004), were from Jackson Laboratories. All mice were maintained in specific-pathogen-free conditions at an Association for Assessment and Accreditation of Laboratory Animal Care-accredited animal facility at the NIAID. All procedures were approved by the NIAID Animal Care and Use Committee (National Institutes of Health, Bethesda, MD).

DTH

Recipient mice were transferred with 2×10^4 T cells from donor mice by i.v. injection. The recipient mice were then immunized with 100μl of emulsion of complete Freund's adjuvant plus 50μg KLH and 25μg ovalbumin 323-339 peptide (OT-II) or Ag85b 240-254 peptide (p25) at the base of the tail the next day. 7 days later after the immunization, ear skin was challenged i.d. with 20μg KLH and/or OVA. Intravital imaging or flow cytometry analysis was performed 48-72 hrs after the challenge.

Blocking antibodies

Rat IgG, anti-PD-L1 (10F.9G2), anti-CTLA4 (UC10-4F10-11) (all from BioXCell), and anti-PD-L2 (3.2) (kindly provided by Gordon J Freeman, Dana-Farber Cancer Institute, Boston, MA), were injected intravenously at 300 μg/mouse one day and one hour before OVA peptide injection.

In vitro T cell stimulation and adoptive transfer

For *in vitro* generated effector T cells, lymph nodes from TCR transgenic mice were disrupted by passage through a 70μm cell strainer (BD Biosciences). 1×10^6 cells were stimulated with 1×10^7 mitomycin C-treated C57BL/6 splenocytes in complete RPMI 1640 (10% FCS, 2mM L-glutamine, 50mM 2-mercaptoethanol, and penicillin plus streptomycin) plus 2μM ovalbumin 323-339 peptide (OT-II) or Ag85b 240-254 peptide (p25) in each well of a 24-well plate. Two days after the stimulation, cells were expanded in the presence of 20U/ml recombinant human IL-2 (R&D systems) and used for experiments 6–7 days post activation. *In vitro* generated effector T cells were labeled with 1μM CMTPX or 100μM cell tracker blue for 15 min at 37 C in HBSS or 10μM CMTMR (Invitrogen) for 15 min at 37°C in complete RPMI. 0.5-1 × 10^7 of each cell type was injected i.v. into recipient animals.

Cell isolation and Flow Cytometry

For skin lymphocyte isolation, ear skin was cut and separated from the cartilage. The separated ears were put into RPMI+1% fetal calf serum containing 0.33mg/ml of Liberase TL (Roche), 0.05% DNase I (Boehringer Mannheim) for 1 hour at 37°C. After the incubation, the tissue was disrupted by passage through a 70μm cell strainer. Cell suspensions were washed and stained with respective antibodies. For analysis of intracellular cytokine production, cell suspensions were obtained in the same manner except that 10μg/ml of BFA (Sigma) was included in the digest buffer and subsequent steps were performed in the presence of 5μg/ml BFA. Cells were surface stained with anti-CD4 eFluor450 (Clone RM4-5), anti-PD-1 PeCy7 (Clone 29F.1A12) (Biolegend), anti-Lag3 PE (Clone eBioC9B7W), anti-Vα2−TCR PE (Clone B20.1), anti-CD3 PeCy7 (Clone 145-2C11), anti-ICAM-1 alexa700 (Clone YN1/1.7.4), anti-LFA-1 PE (Clone M17/4), anti-CD28 PE (Clone 37.51), anti-PD-L1 APC (Clone 10F.9G2), anti-CXCR3 PE (Clone CXCR3-173), anti-CCR4 PeCy7 (Clone 2G12), anti-Vb11 biotin (Clone RR3-15). Cells were fixed with Cytofix buffer, permeabilized with Perm/Wash buffer (BD Biosciences), and stained with anti-IFN-γ Alexa Fluor 647 (Clone XMG1.2) or anti-CTLA4 (Clone UC10-4B9). eGFP was detected in the FITC channel and isotype controls were used to determine background signals for intracellular stains. Flow cytometric data were collected on an LSR II (BD Biosciences) and analyzed with FlowJo software (TreeStar).

Intravital Multiphoton Microscopy

Mice were anesthetized and prepared for intravital 2P imaging. Briefly, the mouse was anesthetized using isoflurane and placed on a custom-designed stage in a heat box. Ear skin was wet with a few drops of PBS and gently placed onto a coverslip and covered with a tape. For acute injection of peptide antigens during imaging, a catheter was placed into the tail vein via a 30GA needle attached to PE-10 tubing (Becton Dickinson) and secured with Durapore Tape (Fischer Scientific). Images were acquired on an LSM 510 NLO multiphoton imaging system (Carl Zeiss Microimaging) or LSM 710 NLO multiphoton imaging system (Carl Zeiss Microimaging), typically 10 z planes spaced 3μm apart every 45 seconds. Fluorescence excitation was provided by a Chameleon Ti:Sapphire laser (Coherent). eGFP and CFP were excited at 920nm or 900nm while CMFDA and CMTPX were excited at 840nm. Raw imaging data were processed with Imaris (Biplane). Automatic object tracking via Imaris Spots was aided with manual corrections to retrieve cell spatial coordinates over time and the resulting data analyzed in MATLAB (MathWorks). AfterEffects (Adobe) or ImageJ software (National Institute of Health) was used to produce video clips.

Statistical analysis

Data were analyzed with GraphPad Prism5 software. *P* values were calculated by the unpaired Student's *t*-test and values of 0.05 or less were considered significant.

Supplementary Material

Refer to Web version on PubMed Central for supplementary material.

Acknowledgements

The authors wish to thank Gordon J Freeman for anti-PD-L2 blocking antibody; Daniel L Barber for PD-1 deficient mice; Naeha Subramanian, Menna Clatworthy, Hai Qi, Marc Bajenoff, and Nathan Peters for helpful discussions and/or technical advice. This work was supported by the Intramural Research Program of NIAID, NIH, the Uehara Memorial Foundation (T.H.), and an HFSP Long-term Fellowship (T.L).

References

Ariotti S, Beltman JB, Chodaczek G, Hoekstra ME, van Beek AE, Gomez-Eerland R, Ritsma L, van Rheenen J, Maree AF, Zal T, et al. Tissue-resident memory CD8+ T cells continuously patrol skin epithelia to quickly recognize local antigen. Proc Natl Acad Sci U S A. 2012; 109:19739–19744. [PubMed: 23150545]

Azar GA, Lemaitre F, Robey EA, Bousso P. Subcellular dynamics of T cell immunological synapses and kinapses in lymph nodes. Proc Natl Acad Sci U S A. 2010; 107:3675–3680. [PubMed: 20133676]

Barnden MJ, Allison J, Heath WR, Carbone FR. Defective TCR expression in transgenic mice constructed using cDNA-based alpha- and beta-chain genes under the control of heterologous regulatory elements. Immunol Cell Biol. 1998; 76:34–40. [PubMed: 9553774]

Bartholomaus I, Kawakami N, Odoardi F, Schlager C, Miljkovic D, Ellwart JW, Klinkert WE, Flugel-Koch C, Issekutz TB, Wekerle H, Flugel A. Effector T cell interactions with meningeal vascular structures in nascent autoimmune CNS lesions. Nature. 2009; 462:94–98. [PubMed: 19829296]

Beattie L, Peltan A, Maroof A, Kirby A, Brown N, Coles M, Smith DF, Kaye PM. Dynamic imaging of experimental Leishmania donovani-induced hepatic granulomas detects Kupffer cell-restricted antigen presentation to antigen-specific CD8 T cells. PLoS Pathog. 2010; 6:e1000805. [PubMed: 20300603]

Bhakta NR, Oh DY, Lewis RS. Calcium oscillations regulate thymocyte motility during positive selection in the three-dimensional thymic environment. Nat Immunol. 2005; 6:143–151. [PubMed: 15654342]

Bousso P, Robey E. Dynamics of CD8+ T cell priming by dendritic cells in intact lymph nodes. Nat Immunol. 2003; 4:579–585. [PubMed: 12730692]

Campbell DJ, Butcher EC. Rapid acquisition of tissue-specific homing phenotypes by CD4(+) T cells activated in cutaneous or mucosal lymphoid tissues. J Exp Med. 2002; 195:135–141. [PubMed: 11781372]

Chodaczek G, Papanna V, Zal MA, Zal T. Body-barrier surveillance by epidermal gammadelta TCRs. Nat Immunol. 2012; 13:272–282. [PubMed: 22327568]

Downey J, Smith A, Schneider H, Hogg N, Rudd CE. TCR/CD3 mediated stop-signal is decoupled in T-cells from Ctla4 deficient mice. Immunol Lett. 2008; 115:70–72. [PubMed: 17964663]

Dustin ML. Stop and go traffic to tune T cell responses. Immunity. 2004; 21:305–314. [PubMed: 15357942]

Egen JG, Allison JP. Cytotoxic T lymphocyte antigen-4 accumulation in the immunological synapse is regulated by TCR signal strength. Immunity. 2002; 16:23–35. [PubMed: 11825563]

Egen JG, Rothfuchs AG, Feng CG, Horwitz MA, Sher A, Germain RN. Intravital imaging reveals limited antigen presentation and T cell effector function in mycobacterial granulomas. Immunity. 2011; 34:807–819. [PubMed: 21596592]

Egen JG, Rothfuchs AG, Feng CG, Winter N, Sher A, Germain RN. Macrophage and T cell dynamics during the development and disintegration of mycobacterial granulomas. Immunity. 2008; 28:271–284. [PubMed: 18261937]

Fife BT, Pauken KE, Eagar TN, Obu T, Wu J, Tang Q, Azuma M, Krummel MF, Bluestone JA. Interactions between PD-1 and PD-L1 promote tolerance by blocking the TCR-induced stop signal. Nat Immunol. 2009; 10:1185–1192. [PubMed: 19783989]

Filipe-Santos O, Pescher P, Breart B, Lippuner C, Aebischer T, Glaichenhaus N, Spath GF, Bousso P. A dynamic map of antigen recognition by CD4 T cells at the site of Leishmania major infection. Cell Host Microbe. 2009; 6:23–33. [PubMed: 19616763]

Gattinoni L, Lugli E, Ji Y, Pos Z, Paulos CM, Quigley MF, Almeida JR, Gostick E, Yu Z, Carpenito C, et al. A human memory T cell subset with stem cell-like properties. Nat Med. 2011; 17:1290–1297. [PubMed: 21926977]

Gebhardt T, Whitney PG, Zaid A, Mackay LK, Brooks AG, Heath WR, Carbone FR, Mueller SN. Different patterns of peripheral migration by memory CD4+ and CD8+ T cells. Nature. 2011; 477:216–219. [PubMed: 21841802]

Germain RN, Robey EA, Cahalan MD. A decade of imaging cellular motility and interaction dynamics in the immune system. Science. 2012; 336:1676–1681. [PubMed: 22745423]

Grossman Z, Paul WE. Adaptive cellular interactions in the immune system: the tunable activation threshold and the significance of subthreshold responses. Proc Natl Acad Sci U S A. 1992; 89:10365–10369. [PubMed: 1438221]

Hafalla JC, Claser C, Couper KN, Grau GE, Renia L, de Souza JB, Riley EM. The CTLA-4 and PD-1/PD-L1 inhibitory pathways independently regulate host resistance to Plasmodium-induced acute immune pathology. PLoS Pathog. 2012; 8:e1002504. [PubMed: 22319445]

Islam SA, Luster AD. T cell homing to epithelial barriers in allergic disease. Nat Med. 2012; 18:705–715. [PubMed: 22561834]

Kawakami N, Nagerl UV, Odoardi F, Bonhoeffer T, Wekerle H, Flugel A. Live imaging of effector cell trafficking and autoantigen recognition within the unfolding autoimmune encephalomyelitis lesion. J Exp Med. 2005; 201:1805–1814. [PubMed: 15939794]

Kearney ER, Pape KA, Loh DY, Jenkins MK. Visualization of peptide-specific T cell immunity and peripheral tolerance induction in vivo. Immunity. 1994; 1:327–339. [PubMed: 7889419]

Kim JV, Kang SS, Dustin ML, McGavern DB. Myelomonocytic cell recruitment causes fatal CNS vascular injury during acute viral meningitis. Nature. 2009; 457:191–195. [PubMed: 19011611]

Lindquist RL, Shakhar G, Dudziak D, Wardemann H, Eisenreich T, Dustin ML, Nussenzweig MC. Visualizing dendritic cell networks in vivo. Nat Immunol. 2004; 5:1243–1250. [PubMed: 15543150]

Linsley PS, Bradshaw J, Greene J, Peach R, Bennett KL, Mittler RS. Intracellular trafficking of CTLA-4 and focal localization towards sites of TCR engagement. Immunity. 1996; 4:535–543. [PubMed: 8673700]

Masters BR, So PT, Buehler C, Barry N, Sutin JD, Mantulin WW, Gratton E. Mitigating thermal mechanical damage potential during two-photon dermal imaging. J Biomed Opt. 2004; 9:1265–1270. [PubMed: 15568947]

Matheu MP, Beeton C, Garcia A, Chi V, Rangaraju S, Safrina O, Monaghan K, Uemura MI, Li D, Pal S, et al. Imaging of effector memory T cells during a delayed-type hypersensitivity reaction and suppression by Kv1.3 channel block. Immunity. 2008; 29:602–614. [PubMed: 18835197]

Mempel TR, Henrickson SE, Von Andrian UH. T-cell priming by dendritic cells in lymph nodes occurs in three distinct phases. Nature. 2004; 427:154–159. [PubMed: 14712275]

Miller MJ, Wei SH, Parker I, Cahalan MD. Two-photon imaging of lymphocyte motility and antigen response in intact lymph node. Science. 2002; 296:1869–1873. [PubMed: 12016203]

Mora JR, Bono MR, Manjunath N, Weninger W, Cavanagh LL, Rosemblatt M, Von Andrian UH. Selective imprinting of gut-homing T cells by Peyer's patch dendritic cells. Nature. 2003; 424:88–93. [PubMed: 12840763]

Muller AJ, Filipe-Santos O, Eberl G, Aebischer T, Spath GF, Bousso P. CD4(+) T Cells Rely on a Cytokine Gradient to Control Intracellular Pathogens beyond Sites of Antigen Presentation. Immunity. 2012; 37:147–157. [PubMed: 22727490]

Negulescu PA, Krasieva TB, Khan A, Kerschbaum HH, Cahalan MD. Polarity of T cell shape, motility, and sensitivity to antigen. Immunity. 1996; 4:421–430. [PubMed: 8630728]

Reinhardt RL, Bullard DC, Weaver CT, Jenkins MK. Preferential accumulation of antigen-specific effector CD4 T cells at an antigen injection site involves CD62E-dependent migration but not local proliferation. J Exp Med. 2003; 197:751–762. [PubMed: 12629067]

Sadik CD, Luster AD. Lipid-cytokine-chemokine cascades orchestrate leukocyte recruitment in inflammation. J Leukoc Biol. 2012; 91:207–215. [PubMed: 22058421]

Sancho D, Vicente-Manzanares M, Mittelbrunn M, Montoya MC, Gordon-Alonso M, Serrador JM, Sanchez-Madrid F. Regulation of microtubule-organizing center orientation and actomyosin

cytoskeleton rearrangement during immune interactions. Immunol Rev. 2002; 189:84–97. [PubMed: 12445267]

Schaefer BC, Schaefer ML, Kappler JW, Marrack P, Kedl RM. Observation of antigen-dependent CD8+ T-cell/ dendritic cell interactions in vivo. Cell Immunol. 2001; 214:110–122. [PubMed: 12088410]

Schaeffer M, Han SJ, Chtanova T, van Dooren GG, Herzmark P, Chen Y, Roysam B, Striepen B, Robey EA. Dynamic imaging of T cell-parasite interactions in the brains of mice chronically infected with Toxoplasma gondii. J Immunol. 2009; 182:6379–6393. [PubMed: 19414791]

Schneider H, Downey J, Smith A, Zinselmeyer BH, Rush C, Brewer JM, Wei B, Hogg N, Garside P, Rudd CE. Reversal of the TCR stop signal by CTLA-4. Science. 2006; 313:1972–1975. [PubMed: 16931720]

Schneider H, Smith X, Liu H, Bismuth G, Rudd CE. CTLA-4 disrupts ZAP70 microcluster formation with reduced T cell/APC dwell times and calcium mobilization. Eur J Immunol. 2008; 38:40–47. [PubMed: 18095376]

Schreiber HA, Hulseberg PD, Lee J, Prechl J, Barta P, Szlavik N, Harding JS, Fabry Z, Sandor M. Dendritic cells in chronic mycobacterial granulomas restrict local anti-bacterial T cell response in a murine model. PLoS One. 2010; 5:e11453. [PubMed: 20625513]

Segel LA, Bar-Or RL. On the role of feedback in promoting conflicting goals of the adaptive immune system. J Immunol. 1999; 163:1342–1349. [PubMed: 10415033]

Stoll S, Delon J, Brotz TM, Germain RN. Dynamic imaging of T cell-dendritic cell interactions in lymph nodes. Science. 2002; 296:1873–1876. [PubMed: 12052961]

Swain SL, McKinstry KK, Strutt TM. Expanding roles for CD4(+) T cells in immunity to viruses. Nat Rev Immunol. 2012; 12:136–148. [PubMed: 22266691]

Utzny C, Coombs D, Muller S, Valitutti S. Analysis of peptide/MHC-induced TCR downregulation: deciphering the triggering kinetics. Cell Biochem Biophys. 2006; 46:101–111. [PubMed: 17012752]

Valitutti S, Coombs D, Dupre L. The space and time frames of T cell activation at the immunological synapse. FEBS Lett. 2010; 584:4851–4857. [PubMed: 20940018]

Vintersten K, Monetti C, Gertsenstein M, Zhang P, Laszlo L, Biechele S, Nagy A. Mouse in red: red fluorescent protein expression in mouse ES cells, embryos, and adult animals. Genesis. 2004; 40:241–246. [PubMed: 15593332]

Waite JC, Leiner I, Lauer P, Rae CS, Barbet G, Zheng H, Portnoy DA, Pamer EG, Dustin ML. Dynamic imaging of the effector immune response to listeria infection in vivo. PLoS Pathog. 2011; 7:e1001326. [PubMed: 21455492]

Wilson EH, Harris TH, Mrass P, John B, Tait ED, Wu GF, Pepper M, Wherry EJ, Dzierzinski F, Roos D, et al. Behavior of parasite-specific effector CD8+ T cells in the brain and visualization of a kinesis-associated system of reticular fibers. Immunity. 2009; 30:300–311. [PubMed: 19167248]

Wolf AJ, Desvignes L, Linas B, Banaiee N, Tamura T, Takatsu K, Ernst JD. Initiation of the adaptive immune response to Mycobacterium tuberculosis depends on antigen production in the local lymph node, not the lungs. J Exp Med. 2008; 205:105–115. [PubMed: 18158321]

Yokosuka T, Takamatsu M, Kobayashi-Imanishi W, Hashimoto-Tane A, Azuma M, Saito T. Programmed cell death 1 forms negative costimulatory microclusters that directly inhibit T cell receptor signaling by recruiting phosphatase SHP2. J Exp Med. 2012; 209:1201–1217. [PubMed: 22641383]

Zhu J, Yamane H, Paul WE. Differentiation of effector CD4 T cell populations (*). Annu Rev Immunol. 2010; 28:445–489. [PubMed: 20192806]

Zinselmeyer BH, Heydari S, Sacristan C, Nayak D, Cammer M, Herz J, Cheng X, Davis SJ, Dustin ML, McGavern DB. PD-1 promotes immune exhaustion by inducing antiviral T cell motility paralysis. J Exp Med. 2013; 210:757–774. [PubMed: 23530125]

Highlights

- Effector $CD4^+$ T cell function and motility inversely correlate in inflamed tissue.
- Antigen sensitivity tuning limits the duration of effector T cell activity *in vivo*.
- PD-1 upregulation contributes to sensitivity loss and cessation of effector function.
- Feedback regulation of effector activity appears to balance peripheral host defense and tissue damage.

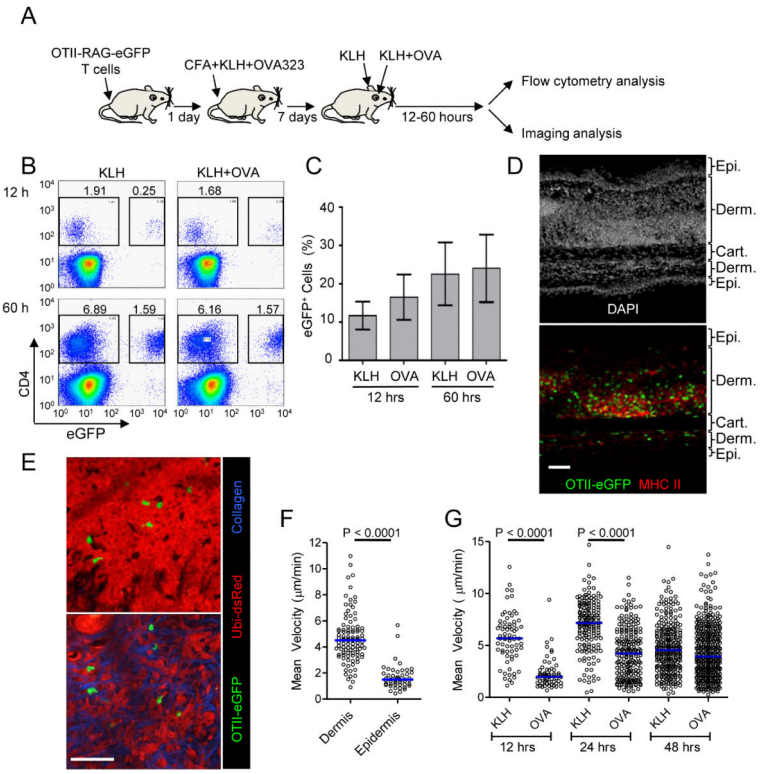

Figure 1. Characterization of antigen-dependent and independent effector T cell behavior in inflamed skin

(A) Schematic illustration of DTH induction. (B) Representative histograms and (C) quantification of $CD4^+eGFP^+$ OT-II T cells from inflamed skin. Ear skin was collected at the indicated time point and cell composition was analyzed by flow cytometry after tissue disruption. Graph shows the percent of $CD4^+$ cells that are $eGFP^+$; mean +/− SD from at least three mice per group. (D) Immunofluorescence staining of an inflamed ear section containing OT-II $eGFP^+$ cells during a DTH response. 48 hrs after KLH challenge, ear skin was fixed, sectioned, and stained with DAPI to identify nuclei and an anti-MHC-II Ab. Epidermis (Epi), dermis (Derm), and cartilage (Cart) regions of the ear are indicated. Note, the side of the ear receiving an intradermal injection of antigen shows the most inflammation and dermal swelling. (E) Representative picture of OT-II T cells in epidermis (upper panel) and dermis (lower panel). See also Movie S1. (F) Comparison of OT-II T cell mean velocity in dermis and epidermis. Each symbol represents an individual cell. Horizontal lines indicate median value of the population. (G) Quantification of mean velocity for dermal OT-II T cells in the presence and absence of cognate antigen. Each symbol represents an individual cell. Horizontal lines indicate median value of the population. P values, unpaired Student's t-test. See also Movie S2. All data are representative of three or more independent experiments. Scale bars: 50μm

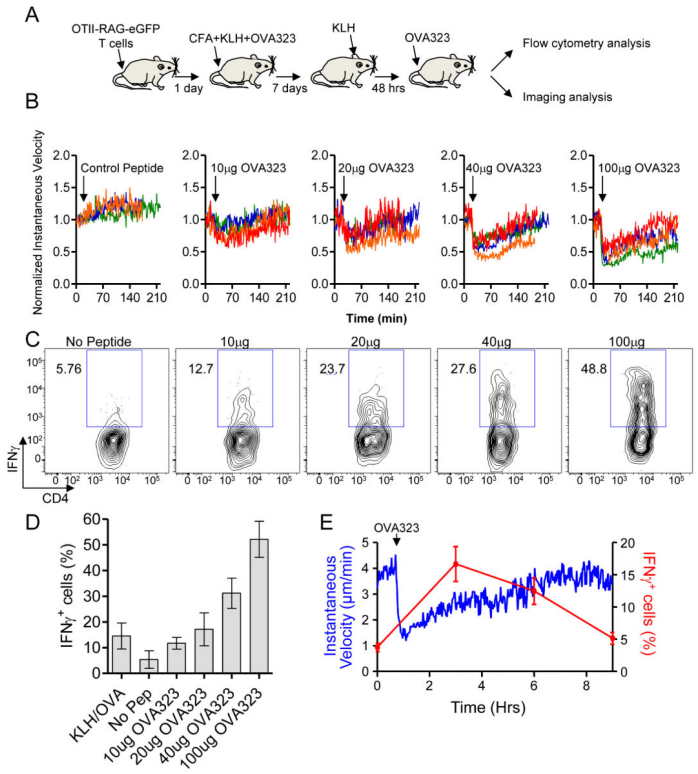

Figure 2. Synchronized activation of effector T cells reveals inverse correlation between effector function and motility

(A) Schematic illustration of modified DTH system. (B) Antigen-induced OT-II T cell arrest in response to different doses of OVA323 peptide. Each line represents the average normalized instantaneous velocity over time from an individual animal treated at a given peptide dose. The velocity before OVA323 peptide administration is normalized to one. Data are compiled from multiple experiments. See also Movie S3. (C) Representative flow cytometry histograms and (D) quantification of IFN-γ production from OT-II T cells 2 hrs after administration of different doses of OVA323 peptide. Graph shows the percent OTII-T cells that are IFN-γ^+; mean +/− SEM from at least 3 mice per group. (E) OT-II T cell instantaneous velocity over time and the percent OT-II T cells that are IFN-γ^+ before and after administration of 100μg of OVA323. See also Movie S4. All data are representative of three or more independent experiments.

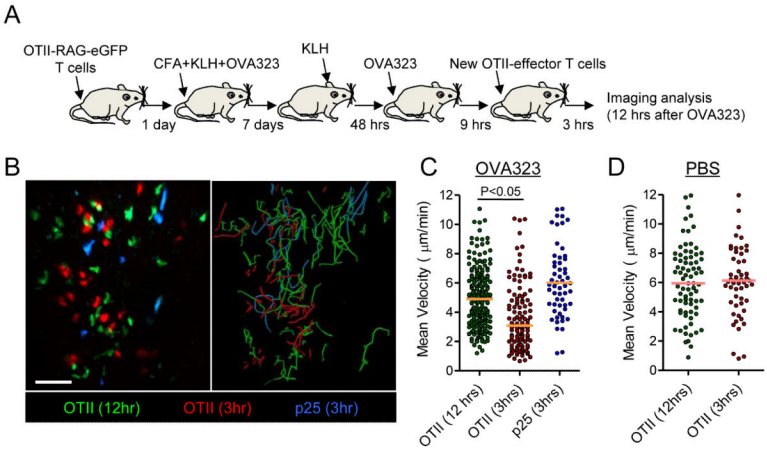

Figure 3. Antigen presentation persists after the regain of T cell motility

(A) Schematic illustration of experimental protocol. (B) Representative image from an intravital data set (left panel). Image was taken 12 hrs after administration of 100μg of OVA323. *In vitro* primed OT-II T cells and p25 T cells were labeled with CMTMR (red) and Cell Tracker blue (blue), respectively, and transferred 3 hrs before image acquisition. Right panel shows the paths of T cell migration over the duration of the movie. See also Movie S5. (C and D) Quantification of mean velocity for endogenously primed OT-II T cells and *in vitro* generated OT-II T cells and p25 T cells. Horizontal lines indicate median value of the population. Data are representative of two independent experiments. Scale bars: 50μm

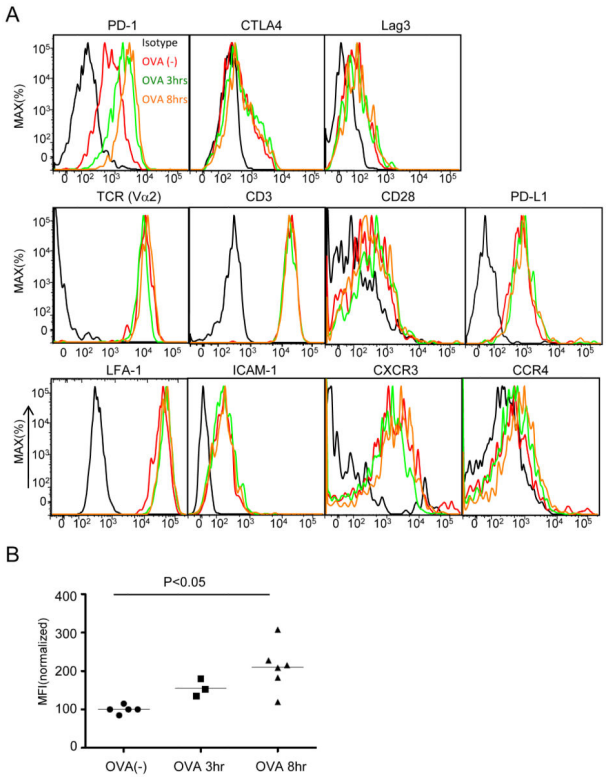

Figure 4. Expression of surface molecules on OT-II T cells after OVA323 administration

(A) Representative histogram of various surface molecules on OT-II T cells from at least three independent experiments. DTH ear skin was collected and digested at the indicated time point after administration of 100μg of OVA323 and cells were surface stained with the indicated antibodies. Intracellular staining was performed for CTLA4. (B) The median fluorescence intensity (MFI) of PD-1 staining was quantified before and after peptide administration. All values were normalized to the average MFI of the OVA(-) group, set as 100. P values, unpaired Student's t-test.

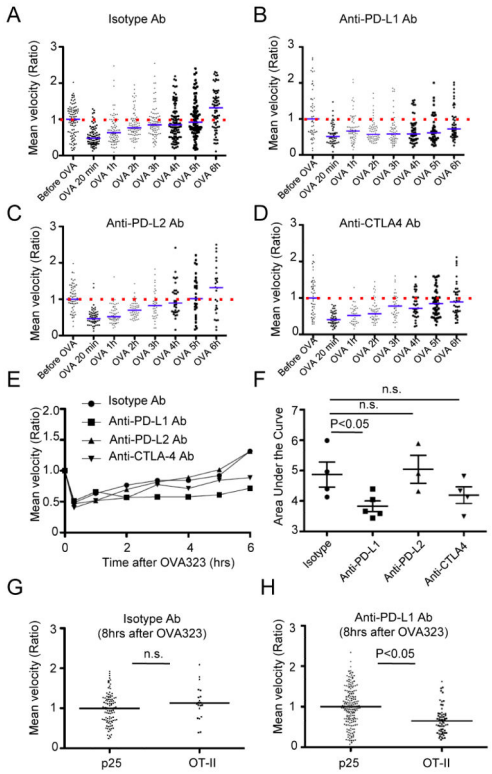

Figure 5. Effect of blocking antibodies on the recovery of T cell motility after OVA323 administration

(A-D) Representative time course of mean velocity for OT-II T cells before and after administration of 100μg of OVA323 in the presence of the indicated antibodies. The median value of the population before OVA323 administration was set as one, and each dot indicates an individual cell. Blue horizontal lines indicate the ratio of mean velocity to initial velocity at the indicated time point, and red dashed lines indicate initial velocity. Data are generated from 30 minute data sets beginning at each indicated time point. (E) Summary of the time course of T cell motility change from data in (A-D). Each symbol indicates the ratio of the mean velocity as in (A-D). (F) Quantification of motility recovery for OT-II T cells in the presence of different blocking antibodies. Area under the curve in (E) was measured. Each symbol indicates area under the curve for an individual independent experiment. (G, H) Comparison of mean velocity between *in vivo* primed p25 T cells and OT-II T cells 8 hrs after OVA 323 stimulation either with isotype antibody treatment (G) or anti-PD-L1 antibody (H). See also Movies S6. Data are representative of three or more independent experiments. P values, unpaired Student's t-test. n.s.- not significant.

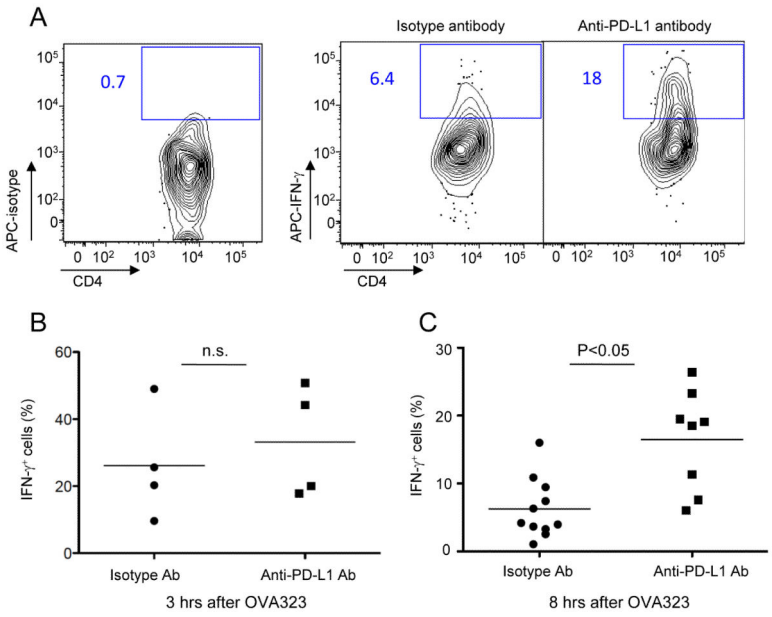

Figure 6. PD-L1 blockade prolongs effector function of OT-II T cells after antigen-induced arrest

(A) Representative contour plots and (B) quantification for IFN-γ production from OT-II T cells in the presence and absence of anti-PD-L1 antibody. DTH was induced in primed mice and the animals treated with isotype control or anti-PD-L1 blocking antibody prior to administration of 100μg OVA323. Skin cells were collected 3 hrs (B) or 8 hrs (A and C) after OVA323 administration and intracellular staining for IFN-γ was performed. Each symbol in (B and C) indicates the result from an individual mouse. Data are representative of three or more independent experiments. P values, unpaired Student's t-test. n.s.- not significant.